Experimental determination of scattering matrices of dust particles at visible wavelengths: IAA light-scattering apparatus

O. Muñoz*, F. Moreno, and D. Guirado

Instituto de Astrofísica de Andalucía, CSIC, Glorieta de la Astronomía s/n, 18080 Granada, Spain.

We present a new laboratory apparatus for measuring the complete scattering matrix as a function of the scattering angle of aerosol particles. The measurements can be performed at the wavelengths of 483, 488, 520, 568, or 647 nm in the scattering angle range from 3° to 177°. The accuracy of the system has been tested by comparison of the measured scattering matrices for water droplets with results of Lorenz-Mie calculations for homogeneous spherical water droplets. The apparatus is devoted to experimentally studying the angle-dependent scattering matrices of dust samples of astrophysical interest. Moreover, there is a great interest in measuring aerosol samples that can affect the radiative balance of the Earth's atmosphere such as desert dust, volcanic ashes, and carbon soot particles.

INTRODUCTION

The study of the scattering behavior of irregular mineral particles is of great importance in many different fields. In particular, irregular dust particles play an important role in the study of the Solar System, especially as far as planetary atmospheres and minor bodies are concerned [1]. If we want to properly interpret space- and ground-based observations we need to know the scattering properties of such irregular mineral particles. For that purpose an experimental apparatus was built in the 1980s in the group of J.W. Hovenier in Amsterdam (see e.g. [2]). In this paper, we present an improved descendant of the Dutch experimental apparatus recently constructed at the Instituto de Astrofísica de Andalucía (IAA) in Granada, Spain [3].

EXPERIMENTAL APPARATUS AND CALIBRATION MEASUREMENTS

In short, to measure the scattering-matrix elements, we use a number of different optical components such as polarizers, a quarter-wave plate, and an electro-optic modulator. These components are used to manipulate the polarization state of light. By using eight different combinations for the orientation angles of the optical components, and assuming reciprocity of the sample, all scattering-matrix elements are obtained as functions of the scattering angle [2]. In the new apparatus, the detectors have been designed so that the blockage of the laser beam at positions close to the forward and backward directions is minimized. This allows us to extend the scattering-angle range of the measurements to 3-177°. Moreover, the accuracy of the measurements at small and large scattering angles has been improved by including in the measuring/reduction process corrections for the background signal. Additionally, we have extended the number of wavelengths of the incident light (λ). In the IAA apparatus, we use a tunable Argon-Krypton laser (483, 488, 520, 568, and 647 nm) as a light source. A detailed description of the instrument and reduction process can be found in [3].

*Corresponding author: Olga Muñoz (olga@iaa.es)

The accuracy and reliability of the instrument is tested by comparing the measured scattering matrices of water droplets at 488 nm, 520 nm, and 647 nm with Lorenz-Mie calculations for a distribution of homogeneous water droplets. For the Lorenz-Mie calculations, we assume a log-normal size distribution as defined by [4]. The refractive index of water is assumed as a fixed parameter at the three studied wavelengths (m=1.33-0.0i). The method to find the best-fitted values for r_g and σ_g that define the log-normal size distribution, is based on the downhill simplex method of Nelder and Mead [5], particularly the FORTRAN implementation described in the Numerical Recipes book [6], subroutine AMOEBA. The method is independently applied to fit the $F_{11}(\theta)$ and $-F_{12}(\theta)/F_{11}(\theta)$ at the 3 studied wavelengths, namely 488, 520, and 647 nm. The averaged values obtained from the best fits for the six studied functions give a value of $\sigma_a = 1.50 \pm 0.04$ and $r_a = 0.80 \pm 0.07$ μm.

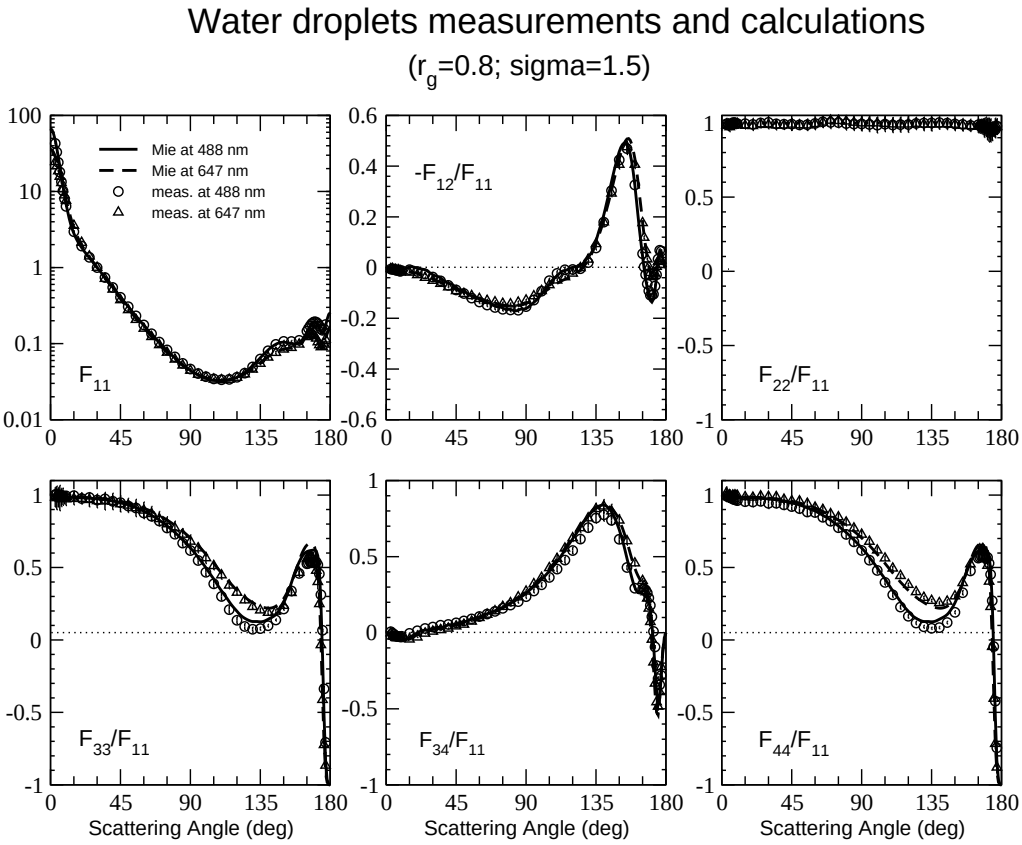

Figure 1. Measured scattering matrix for water droplets at λ=488 nm (circles) and 647 nm (triangles). Solid and dashed lines correspond to results of Lorenz-Mie calculations at 488 nm and 647 nm, respectively, for a log-normal size distribution ($r_g = 0.84$ μm, and σ_g=1.5). Errors are presented by bars that sometimes are not seen because they are smaller than the symbols.

As an example, in Fig. 1, we present the measured and calculated scattering matrices as functions of the scattering angle at $\lambda = 488$ nm and 647 nm. The measured and calculated $F_{11}(\theta)$ are plotted on a logarithmic scale and normalized to 1 at 30°. The other

matrix elements are plotted relative to $F_{11}(\theta)$. We refrain from showing the four element ratios $F_{13}(\theta)/F_{11}(\theta)$, $F_{14}(\theta)/F_{11}(\theta)$, $F_{23}(\theta)/F_{11}(\theta)$, and $F_{24}(\theta)/F_{11}(\theta)$, since we verified that these ratios do not differ from zero by more than the error bars, in accordance with Lorenz-Mie theory. The measurements satisfy the Cloude coherency matrix test (see e.g. [7]) at all measured scattering angles. As shown, the water droplets measurements show an excellent agreement with the Lorenz-Mie computations over the entire angle range at the two presented wavelengths. The experimental data exhibit the typical behavior of a distribution of homogeneous spherical particles, i.e., $F_{22}(\theta)/F_{11}(\theta)$ is equal to unity at all scattering angles. In addition, the $F_{33}(\theta)/F_{11}(\theta)$ and $F_{44}(\theta)/F_{11}(\theta)$ ratios are identical to one another at all scattering angles.

SCATTERING MATRICES FOR A SAMPLE OF WHITE CLAY PARTICLES

As an example of measurements with dust particles, in Fig. 2, we present the measured scattering-matrix elements as a function of the scattering angle of a sample of white clay particles. The measurements are performed at 488 and 647 nm. The scattering matrices fulfill the Cloude coherency matrix test within the experimental errors at all measured scattering angles (see e.g. [7]). The size distribution of the sample has been measured by a Mastersizer 2000, Malvern instruments. The retrieved size distribution parameters based on diffraction are $r_{\text{eff}} = 1.39$ µm and v_{eff}=1.56 [4]. As mentioned above, the measured phase functions are normalized to 1 at 30°. The measured scattering matrix elements present the typical behavior of irregular mineral particles (see e.g. [8] and the Amsterdam Light Scattering Database, www.astro.uva.nl/scatter). The measured $F_{11}(\theta)$ elements present a strong forward peak and almost no structure at side- and backscattering angles. The degree of linear polarization for unpolarized incident light, $-F_{12}(\theta)/F_{11}(\theta)$, presents the typical bell-shape with a maximum around 90° and a negative branch at large scattering angles. The $F_{44}(\theta)/F_{11}(\theta)$ ratios are larger than the $F_{33}(\theta)/F_{11}(\theta)$ at scattering angles larger than 100°, whereas the $F_{22}(\theta)/F_{11}(\theta)$ ratio is different from unity at nearly all measured scattering angles.

When comparing the measurements at the two studied wavelength we observe that the maximum of the degree of linear polarization increases when increasing the wavelength of the incident light, i.e., the smaller the size parameter, the higher the maximum of the degree of linear polarization. Moreover, the measured $F_{22}(\theta)/F_{11}(\theta)$ ratio at 647 nm shows the highest values at almost all measured scattering angles. In contrast, the $F_{33}(\theta)/F_{11}(\theta)$, $F_{34}(\theta)/F_{11}(\theta)$, and $F_{44}(\theta)/F_{11}(\theta)$ ratios do not seem to show any significant differences at the two wavelengths studied. Similar wavelength dependence showed up in the previous measurements performed in Amsterdam with red and green clay particles ([8, 9] and `http://www.astro.uva.nl/scatter`).

REFERENCES

[1] J.W. Hovenier and O. Muñoz. Light scattering in the Solar System: An introductory review. JQSRT **110**(14–16) (2009).

[2] J.W. Hovenier. Measuring scattering matrices of small particles at optical wavelengths. In: *Light scattering by nonspherical particles*. M.I. Mishchenko, J.W. Hovenier and L.D. Travis (eds.). Academic, San Diego, CA (2000).

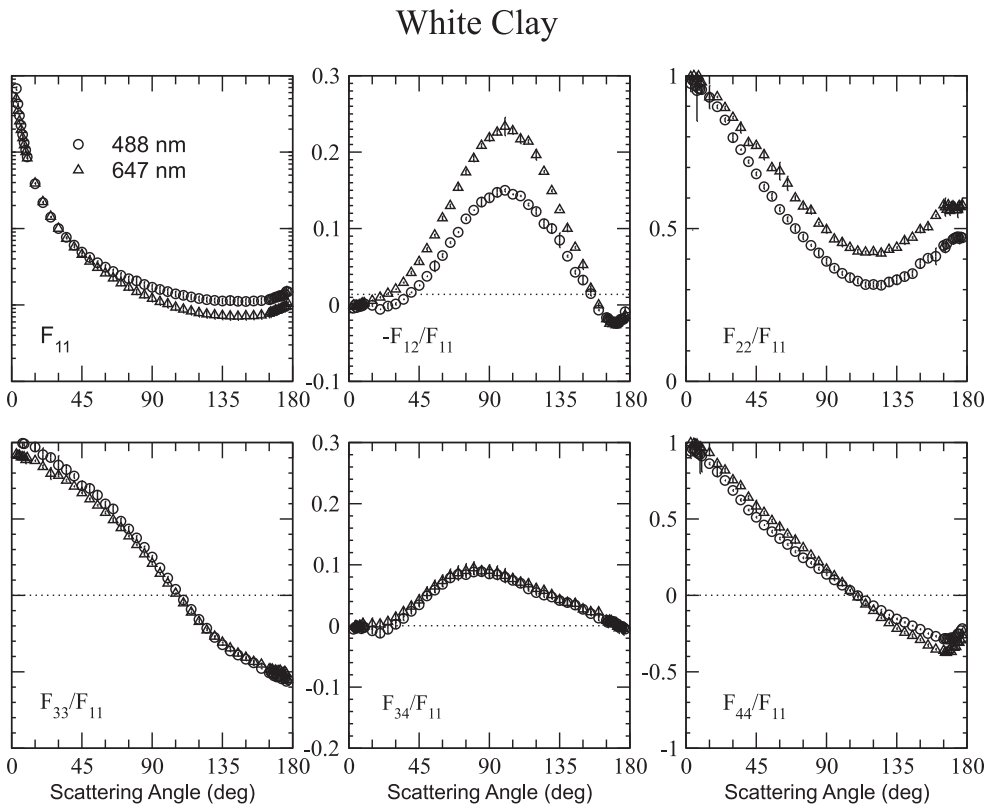

Figure 2. Measured scattering matrix elements for a sample of white clay particles at two different wavelengths 488 nm (circles) and 647 nm (triangles). The measurements are presented together with their error bars. In case no error bars are shown, they are smaller than the symbols.

[3] O. Muñoz et al. The new IAA Light scattering apparatus. JQSRT **111** (2010).

[4] J.E. Hansen, L.D. Travis. Light scattering in planetary atmospheres. Space Sci. Rev. **16**(4) 1974.

[5] A. Nelder and R.A. Mead. A simplex method for function minimization. Computer Journal **7** (1965).

[6] W. Press, S. Teukolsky, W. Vetterling and B. Flannery. *Numerical Recipes in Fortran 77, second edition*. ISBN 0-521-43064-X (1992).

[7] J.W. Hovenier, C.V.M. van der Mee and H. Domke. *Transfer of polarized light in planetary atmospheres : Basic concepts and practical methods*. Kluwer Springer, Dordrecht (2004).

[8] H. Volten, O. Muñoz, E. Rol, J.F. de Haan, V. Vassen, J.W. Hovenier, K. Muinonen and T. Nousiainen. Scattering matrices of mineral aerosol particles at 441.6 nm and 632.8 nm. J. Geophys. Res. **106** (2001).

[9] O. Muñoz, H. Volten, J.F. de Haan, W. Vassen, and J.W. Hovenier. Experimental determination of scattering matrices of randomly oriented fly ash and clay particles at 442 and 633 nm. J. Geophys. Res. **106** (2001)